Hindawi
Science and Technology of Nuclear Installations
Volume 2018, Article ID 4163914, 8 pages
https://doi.org/10.1155/2018/4163914

Research Article

Moisture Transfer Model and Simulation for Dehumidification of HTGR Core

Jun Li,[1,2] **Zhenzhong Zhang**,[1] **Yingchao Meng**,[1] **Huaqiang Yin**,[1] **Shengchao Ma**,[1] **Xuedong He**,[1] **Xingtuan Yang**,[1] **and Shengyao Jiang**[1]

[1]*Institute of Nuclear and New Energy Technology, Collaborative Innovation Center of Advanced Nuclear Energy Technology, Key Laboratory of Advanced Reactor Engineering and Safety of Ministry of Education, Tsinghua University, Beijing 100084, China*
[2]*Nuclear Power Institute of China, Chengdu 610231, China*

Correspondence should be addressed to Huaqiang Yin; yinhuaqiang@tsinghua.edu.cn

Received 6 June 2018; Accepted 25 July 2018; Published 5 August 2018

Academic Editor: Eugenijus Uščuras

A large number of carbon materials are adopted in high-temperature gas-cooled reactor (HTGR). These carbon materials mainly include graphite IG-110 and boron-containing carbon material (BC), both of which are typical porous materials and normally absorb moisture. In order to inhibit the chemical corrosion reaction between core internals materials and moisture, the core needs to be strictly dehumidified before the reactor is put into operation. This paper mainly analyzed the moisture transfer mechanism in these carbon materials. Moisture transfer models were developed, and the dehumidification process of HTR-PM core was simulated. In addition, the influence of working temperature and system pressure on dehumidification was studied as well.

1. Introduction

Due to the excellent comprehensive performance of carbon materials, they have been extensively adopted in high-temperature gas-cooled reactor (HTGR), serving as structural material, fuel matrix material, etc. [1–3]. These carbon materials used in HTGR typically include isostatic pressure graphite IG-110 and boron-containing carbon material (BC) [4]. Graphite IG-110 mainly serves as fuel matrix material, neutron reflecting layer, and other reactor core internals, while for BC, since it contains boron, which has a big neutron absorption cross section, it is made into the shielding layer [5]. It has been reported that about 60 tons and 1000 tons of graphite have been applied in 10 MW high-temperature gas-cooled reactor (HTR-10) [6] and high-temperature gas-cooled reactor-pebblebed modules (HTR-PM) [7], respectively.

As porous material, carbon materials have numerous pore structures and large specific surface area. The pore structures and molecule groups attached on the surface of pores result in strong moisture absorption capacity [8, 9]. Also, other impurities, such as H_2O, O_2, and CO_2, can be absorbed by carbon materials as well. These impurities will react with the carbon materials at high temperature, thus, weakening the material strength and decreasing the service life of HTGR [10–13]. In addition, under some extreme nuclear accidents, e.g., air or water leakage accident, the corrosion can be even more serious [14, 15]. In order to attenuate the corrosion, the limited value of moisture content in the helium coolant of the primary circuit is set as 2 cm^3/m^3 [16]. Therefore, before power operation and test, the reactor internals and fuel balls need to be dehumidified to control the moisture content to a certain level.

The dehumidification system [17] of HTR-PM is shown in Figure 1. Firstly, the primary circuit is evacuated and then filled with coolant helium at pressure of 7 MPa. The circulated helium is driven by helium circulator, whose mechanical energy is transformed into heat of helium. Thus, the temperature of helium can be heated to 250°C. Due to the high temperature, moisture absorbed in the carbon internals of reactor core will be released and then carried away by flowing helium. The helium flow containing relatively high moisture content will flow out of internals and then be cooled to about 20°C in two water-helium coolers, so the water

Table 1: Expressions of D_0 according to diffusion type and gas component.

Kn	Diffusion type	Gas component	D_0
$Kn < 0.1$	general diffusion [21]	unitary gas	$D_F = \frac{1}{3}\lambda\sqrt{\frac{8RT}{\pi M}}$
		binary gas	$D_{AB} = \frac{4.36 \times T^{1.5}(1/M_A + 1/M_B)^{0.5}}{10^4 \times P(\nu_A{}^{1/3} + \nu_B{}^{1/3})^2}$
$0.1 < Kn < 10$	Knudsen diffusion	-	$D_K = \frac{1}{3}d\sqrt{\frac{8RT}{\pi M}}$
$Kn > 10$	transition diffusion	-	$D_T = \frac{1}{1/D_F + 1/D_K}$ or $\frac{1}{1/D_{AB} + 1/D_K}$

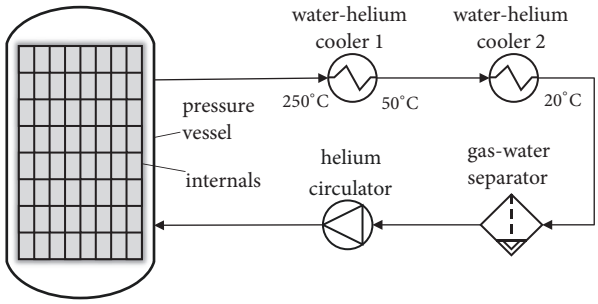

Figure 1: Dehumidification system of HTR-PM.

vapor will condense to liquid water which can be separated in gas-water separator. Finally, dry helium will return to the reactor core. This circulation of helium flow described above will gradually decrease the moisture content in the carbon internals. After being dehumidified for several dozens of days, the moisture content of reactor core will meet the design requirement.

Dehumidification process mainly includes moisture transfer in carbon materials, moisture transfer in helium flow, and the condensation and separation of moisture. During dehumidification and purification process of reactor core, mass transfer in carbon material is considered as the dominating factor. Thus, mass transfer behavior in these carbon materials is worth investigating.

In this paper, Section 2 will present the analysis on moisture transfer mechanism in carbon materials, and then mathematical models will be developed in Section 3. In Section 4, the simulation on dehumidification of HTR-PM will be introduced, and simulation result will be analyzed.

2. Moisture Transfer Mechanism

2.1. Mass and Heat Transfer. Dehumidification process of porous material involves both moisture mass transfer and heat transfer, the relationship of which can be described by Lewis Number Le:

$$Le = \frac{\alpha}{D} \tag{1}$$

where α (m^2/s) and D (m^2/s) are heat diffusion coefficient and mass diffusion coefficient respectively.

While $Le > 60$, it is thought that the heat transfer is faster much more than mass transfer, so that it can be neglected in the analysis [18]. For graphite, the heat diffusion coefficient is about 1.07×10^{-4} m^2/s, and mass diffusion coefficient ranges $10^{-7} \sim 10^{-6}$ m^2/s. Thus, Le of graphite ranges $10^2 \sim 10^3$, which means that the heat transfer can be neglected, so it is thought that the mass transfer takes place at constant temperature in analysis.

Considering the moisture in material is in gaseous state, the mass transfer mechanism of gas in porous material involves molecular diffusion and seepage flow.

2.2. Molecular Diffusion. Molecular diffusion is the result of molecular thermal motion and collision, the mass flux density $\boldsymbol{J}$ ($kg \cdot m^{-2} \cdot s^{-1}$) caused by which can be described by Fick's law:

$$\boldsymbol{J} = -D_e \nabla \rho \tag{2}$$

where ρ (kg/m^3) is moisture concentration and D_e (m^2/s) is effective diffusion coefficient. D_e is influenced by diffusion type, gas component, porosity of material and tortuosity of pore, etc. D_e can be expressed as

$$D_e = D_0 \times \frac{\varepsilon_e}{\tau} \tag{3}$$

where D_0 (m^2/s) is the gas diffusion coefficient. ε_e is effective porosity of material, which is equal to open porosity in general. τ is tortuosity of pore, which is defined as the ratio of the actual length to the apparent length of pore. In addition, the tortuosity is in reciprocal relationship to the effective porosity; thus, relation $\tau = \varepsilon_e{}^{-1}$ has been adopted to the analysis of graphite [19, 20]. Table 1 summarizes the expressions of D_0 according to diffusion type and gas component.

In Table 1, P (Pa) is the gas pressure, T (K) is the temperature, and R is gas constant which is 8.314 J/(mol·K) in general. M_A (g/mol) and M_B (g/mol) are the molar mass of gas component A and B, respectively. ν_A (m^3/kmol) and ν_B (m^3/kmol) are the molar volume of component A and B respectively, which are in liquid state and at normal boiling point.

Diffusion type is influenced by pore diameter d and molecular average free path λ, which can be determined by Knudsen number Kn. Kn can be expressed as

$$Kn = \frac{\lambda}{d} \tag{4}$$

Table 2: Pore parameters of carbon materials.

Parameter	IG-110	BC
Volume density/ (g/cm^3)	1.7435	1.6960
Total porosity ε_t/%	22.85	25.61
Open porosity ε_o/%	19.68	14.37
Closed porosity ε_c/%	3.17	11.24
Specific surface area/ (m^2/g)	15.93	7.34
Most probable pore diameter d/nm	2512	30262

where d is also the most probable pore diameter of material. The value of Kn and corresponding diffusion type are presented in Table 1. λ can be expressed as [22]

$$\lambda = \frac{3.2\mu}{P}\sqrt{\frac{RT}{2\pi M}} \tag{5}$$

where μ (Pa·s or kg/(m·s)) is the kinetic viscosity of gas, P (Pa) is the pressure, and M (kg/mol) is the molar mass. Relevant parameters of material IG-110 and BC, which are acquired by mercury intrusion porosimetry (MIP), are shown in Table 2.

2.3. Seepage. Besides molecular diffusion, another possible transfer mechanism is convection, which can be defined as seepage in porous media. Seepage flow is a kind of viscous flow driven by pressure gradient. According to Darcy's law, the seepage velocity $\boldsymbol{u}$ (m/s) is

$$\boldsymbol{u} = -\frac{K}{\mu}\nabla P \tag{6}$$

where K (m^2) is the permeability of porous material, which is influenced by porosity, pore diameter, tortuosity, etc. According to Timur formula [23], $K \propto {\varepsilon_e}^{4.4}$. In addition, research has shown that, for graphite, whose open porosity is about 10%, K is around 10^{-16} m^2 [24].

2.4. Comparison of Transfer Mechanisms at Different Pressure. Different drying methods involve different pressure conditions. For the dehumidification of HTR-PM, the pressure of its working atmosphere P_o (Pa) is 7 MPa, while for vacuum drying method and hot air drying method which are extensively adopted in experiment and industry, P_o is vacuum and 0.1 MPa, respectively. The working pressure has a great influence on the moisture transfer mechanism in porous materials. A comparison is given in Table 3. In addition, the comparison is based on the following conditions: temperature is 250°C, the working atmosphere is helium, and the initial moisture content $C_{r,0}$ is 0.1%. Moisture content C_r is defined as

$$C_r = \frac{m_{H2O}}{m_C} \times 100\% \tag{7}$$

where m_C (kg) is the dry material mass and m_{H2O} (kg) is the moisture mass. In addition, both of the density of IG-100 and BC are set to 1700 kg/m^3 in analysis.

The comparison is discussed as follows. For hot air drying method, where P_o = 0.1 MPa, the gas mixture in pores of material is binary, which consists of H_2O and He. The released moisture can generate a high pressure P_i in pores, which can be 2.86 MPa in early stage as if all the absorbed moisture transforms to vapor. Then the pressure gradient between P_i and P_o drives the seepage flow in pores. Meanwhile, molecular diffusion also exists. According to (5), molecular free path λ of H_2O is about 114 nm (250°C, 0.1 MPa), while the most probable pore diameters d of IG-110 and BC are 2.5 μm and 30.3 μm, respectively, so $Kn < 0.1$, which means that the general diffusion dominates in pores. As for vacuum drying method, where $P_o < 0.1$ MPa, only water vapor exists in pores and Knudsen diffusion also exists according to Kn. As for the dehumidification of HTR-PM, where P_o = 7 MPa, seepage flow driven by the pressure gradient can be neglected and P_i can be considered constant; thus the gas diffusion coefficient D_0 influenced by P_i is constant as well.

3. Mathematical Model

Two mathematical models for moisture transfer, diffusion model and diffusion-seepage model, are developed and presented here. In addition, the gas components in the equations below include H_2O and He.

3.1. Diffusion Model. Diffusion model is based on molecular diffusion and Fick's law. The governing equation for moisture mass in porous material is

$$\frac{\partial \rho_{H_2O}}{\partial \tau} = -\nabla \boldsymbol{J} = D_e \nabla^2 \rho_{H_2O} \tag{8}$$

where ρ_{H2O} (kg/m^3) is moisture concentration.

3.2. Diffusion-Seepage Model. Diffusion-seepage model is based on diffusion and seepage, and the corresponding governing equation of moisture is

$$\frac{\partial \rho_{H_2O}}{\partial \tau} = \nabla\left(\frac{KRT\cdot\rho_{H_2O}}{\mu_{He+H_2O}\cdot M_{He+H_2O}}\cdot\nabla\rho_{He+H_2O} + D_e\nabla\rho_{H_2O}\right) \tag{9}$$

where M_{He+H2O} (kg/mol), μ_{He+H2O} (Pa·s or kg/(m·s)), and ρ_{He+H2O} (kg/m^3) are the molar mass, kinetic viscosity, and density of binary gas consists of H_2O, and He, respectively.

The kinetic viscosity of binary gas is [25]

$$u_{He+H_2O} = \frac{a_{H_2O}{M_{H_2O}}^{0.5}u_{H_2O} + a_{He}{M_{He}}^{0.5}u_{He}}{a_{H_2O}{M_{H_2O}}^{0.5} + a_{He}{M_{He}}^{0.5}} \tag{10}$$

where a_{H2O} and a_{He} are the volume percentages of H_2O and He, respectively.

For the binary gas at 0.1 MPa, due to the relatively small proportion of He in pore, it has little effect on moisture transfer. Therefore, to simplify the governing Equation (9), ρ_{He} can be considered as a constant and then the simplified equation is

$$\frac{\partial \rho_{H_2O}}{\partial \tau} = \nabla\left[\left(\frac{KRT\cdot\rho_{H_2O}}{\mu_{He+H_2O}\cdot M_{He+H_2O}} + D_e\right)\nabla\rho_{H_2O}\right] \tag{11}$$

Table 3: Comparison of transfer mechanisms at different pressure.

P_o/MPa	< 0.1 (vacuum)	0.1 (normal pressure)	7 (high pressure)
Moisture transfer mechanism	diffusion +seepage	diffusion + seepage	diffusion
Gas component	H_2O	H_2O + He	H_2O + He
Diffusion type	general diffusion + Knudsen diffusion	general diffusion	general diffusion
Gas diffusion coefficient D_0	variable	variable	constant

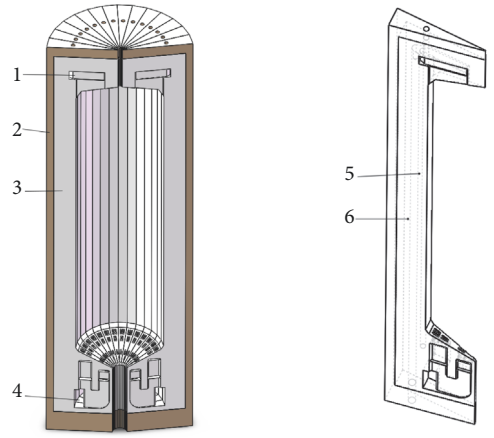

1. cold gas chamber
2. insulation layer
3. reflecting layer
4. hot gas chamber
5. control rod channel
6. cold gas channel

(a) Part of internals

(b) A module of internals

Figure 2: Internals in HTR-PM core.

4. Simulation and Result Analysis

4.1. Initial Parameters and Boundary Conditions. The dehumidification process of HTR-PM core has been simulated by using COMSOL Multiphysics software. Table 3 and (8) demonstrate the corresponding physical hypothesis and mathematical model, respectively.

The geometric model of HTR-PM core is shown in Figure 2. The internals in HTR-PM core mainly include the reflecting layer and insulation layer. Reflecting layer, mainly made of graphite bricks (IG-110), can be approximately considered as a cylinder, the dimension of which is 15600 mm in height and 4500 mm in outside diameter. In addition, the reflecting layer creates an interior space to contain fuel balls, the dimension of which is 11800 mm in equivalent height and 3000 mm in inside diameter. Insulation layer, mainly made of carbon bricks (BC), is also an approximate cylinder located outside the reflecting layer, the dimension of which is 4500 mm in inside diameter and 5000 mm in outside diameter. In addition, the thickness of top and bottom insulation layers is 400 mm and 800 mm, respectively. In fact, the horizontal cross section is not a perfect round but a regular polygon with 30 edges. Moreover, diameter of fuel ball is 60 mm. During the dehumidification process, the helium flow (250°C, 7 MPa) takes the moisture away from internals. Helium flows up from core bottom to cold gas chamber through cold gas channel and then flows down to hot gas chamber through core chamber and leaves the core at last.

Some simplifications of geometric model are adopted here. The neutron source channels, absorption ball channels, hot gas duct, dowels and keys, gap between graphite and carbon bricks, and so on are neglected. Thus, the internals model can be divided into 30 same trigonal prism modules, one of which is shown in Figure 2(b). Each module is mirror symmetrical to the adjacent one. Therefore, we can adopt only one module to represent the moisture transfer process in the whole core internals. In addition, pore structure of materials features isotropy, and the material parameters of fuel ball are considered the same as graphite IG-110.

The mass transfer process is considered as internal diffusion controlled, so the first kind of boundary condition is adopted to the model, which means moisture content $C_{r,b}$ on the boundary, surface of which is exposed to helium atmosphere, is constant. Then $C_{r,b} = 0$ is adopted in this simulation. In addition, the kinetic viscosity u of gas is considered constant due to the very small effect of pressure variation.

Some key parameters adopted in simulation are presented in Table 4.

4.2. Result Analysis of Simulation. According to the numerical simulation, the distribution of moisture content C_r (%) in HTR-PM core at time t = 50 d is shown in Figure 3, where d represents units day. It can be found from Figure 3(a) that moisture mainly concentrates at the top, bottom, and

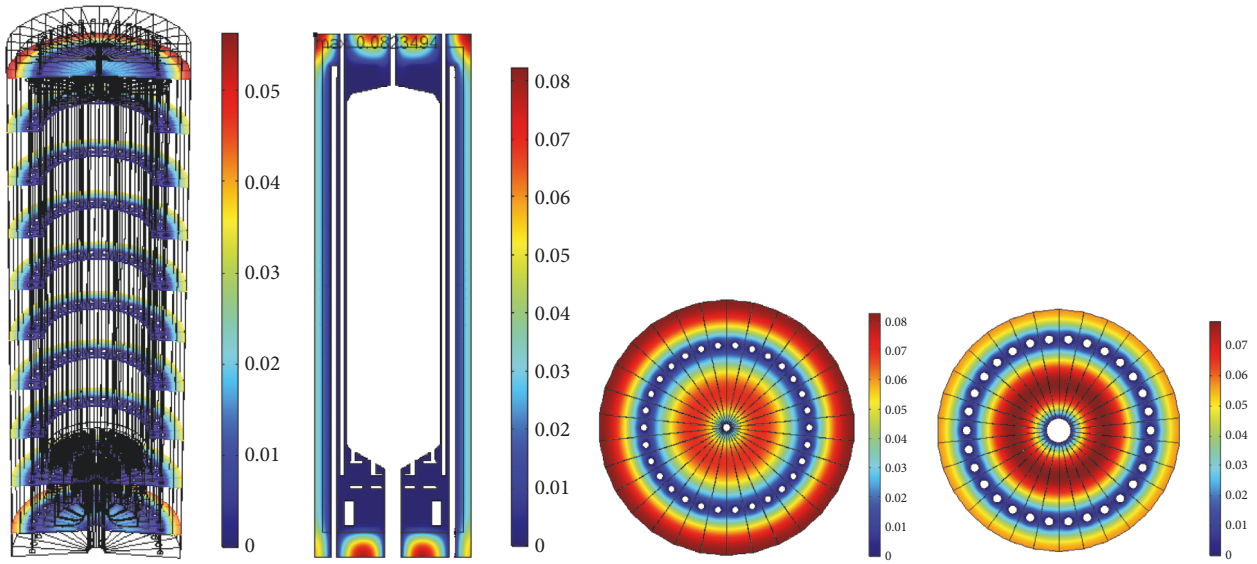

(a) Horizontal cross sections (b) Axial cross section (c) Top surface (d) Bottom surface

FIGURE 3: Distribution of C_r (%) in HTR-PM core (t = 50 d).

TABLE 4: Some parameters of model (250°C, 7 MPa).

Parameter	Value	Unit
Density of helium ρ_{He}	6.524	kg/m^3
Molar mass of He	0.004	kg/mol
Molar mass of H_2O	0.018	kg/mol
Kinetic viscosity of helium u_{He}	2.925×10^{-5}	kg/(m·s)
Kinetic viscosity of water vapor u_{H2O}	1.822×10^{-5}	kg/(m·s)
Most probable aperture of BC	30.3	μm
Most probable aperture of IG-110	2.5	μm
Open porosity of BC ε_o	14.37	%
Open porosity of IG-110 ε_o	19.68	%
Gas diffusion coefficient D_{AB} of binary gas (H_2O + He)	1.226×10^{-6}	m^2/s
Effective diffusion coefficient D_e	$D_e=D_{AB}\times\varepsilon_o^2$	m^2/s
Permeability K of BC	0.49×10^{-15}	m^2
Permeability K of IG-110	1.97×10^{-15}	m^2

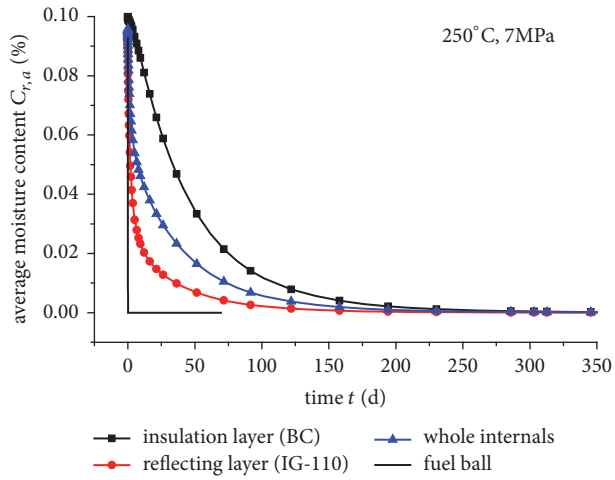

FIGURE 4: Curves of moisture versus time.

side of core. Figure 3(b) presents the moisture distribution at the axial cross section. It can be found that the maximum C_r locates at the top of core. In addition, Figure 3(c) and Figure 3(d) further demonstrate the moisture distribution at the top and bottom surface, respectively. It can be seen that C_r near the cold gas and control rod channels, fuel feed tube, and fuel discharge tube is relatively low, while it is much higher elsewhere.

The curves of moisture content versus time are shown in Figure 4. It can be found that the average moisture content $C_{r,a}$ of internals and fuel ball decreases exponentially, in which it can be explained that moisture content decreases much faster in the early stage because of the high moisture concentration gradient and decreases slower in the later stage as a result of the decrease of concentration gradient. $C_{r,a}$ of fuel ball decreases far faster than that of core internals. Thus, the internals, not fuel balls, are the major limiting factor for the dehumidification. It can also be found that the required time to reach $C_{r,a}$ = 0.02%, 0.01%, and 0.005% of whole internals is 43 d, 72 d, and 108 d, respectively. In addition, $C_{r,a}$ of reflecting layer (IG-110) decreases much faster than that of insulation layer (BC), which can be attributed to the larger open porosity ε_o of IG-110. Thus effective diffusion coefficient D_e of IG-110 is much larger, which promotes the moisture transfer.

4.3. Sensitivity Analysis. In order to accelerate the moisture transfer to improve the dehumidification efficiency, it is

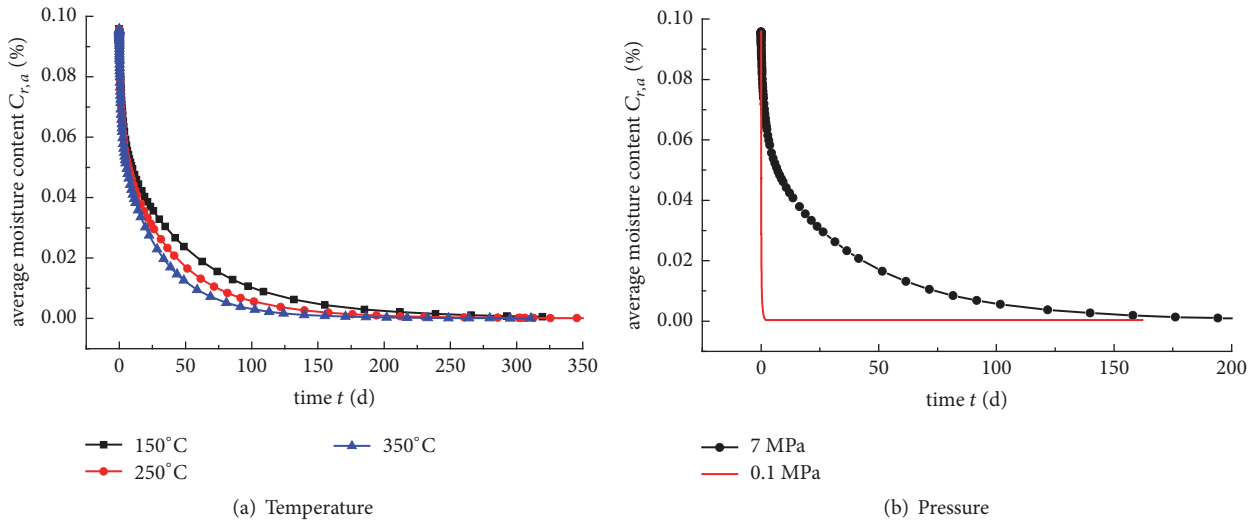

(a) Temperature (b) Pressure

Figure 5: Curves of moisture versus time at different temperature and pressure.

reasonable to promote the molecular diffusion and seepage flow. According to the relations, $D_e \propto T^{1.5}$ and $D_e \propto P^{-1}$, molecular diffusion can be promoted by increasing the temperature T and decreasing the system pressure P_o, while seepage can be promoted by increasing the pressure gradient, which can be achieved by decreasing the system pressure P_o.

The influence of temperature T on dehumidification of HTR-PM is shown in Figure 5(a), where $C_{r,a}$ on Y-axis denotes the average moisture content of whole internals obtained by simulation. It can be found that the dehumidification efficiency increases as temperature increases. Figure 5(b) presents the influence of system pressure P_o on dehumidification, and it shows that the dehumidification efficiency of 0.1 MPa is certainly much higher than that of 7 MPa. In addition, in the simulation where $P_o = 0.1$ MPa, the diffusion-seepage model is adopted and D_e is considered constant to simplify the computation.

As for the actual dehumidification for HTR-PM, $T = 250^\circ$C and $P_o = 7$ MPa. Since the temperature is already pretty high, the promotion by increasing temperature is limited, while as for the system pressure, if it is reduced greatly from 7 MPa to 0.1 MPa, this change will promote both the diffusion and seepage significantly. But on the other hand, the decrease of pressure is not advantageous for the core to be heated. It is because the heat of core is transformed from mechanical energy of helium circulator; thus the heating power is relatively low at low pressure.

4.4. Analytical Solution. In order to obtain an analytical solution of the mathematical model, the irregular geometric model of core internals can be represented by an infinite plate, whose characteristic length L_c (m) is the same as that of irregular geometry. In addition, $L_c = V/A_e$, where V (m^3) and A_e (m^2) are the volume and effective surface area of geometry, respectively.

The infinite plate with $2L_c$ thickness is shown in Figure 6. Diffusion model (8) is adopted. The moisture content is

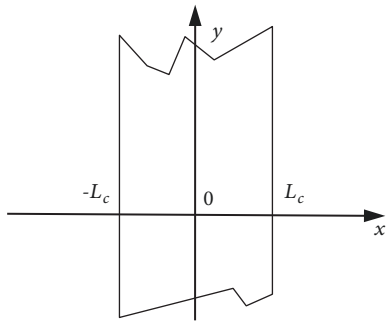

Figure 6: Infinite plate.

$C_r(x,t)$, and effective diffusion coefficient D_e is constant. Thus, the governing equation can be rewritten as

$$\frac{\partial C_r}{\partial t} = D_e \frac{\partial^2 C_r}{\partial x^2} \tag{12}$$

The boundary condition is $C_r(x = L_c, t) = C_{r,b}$. The initial condition is $C_r(x, t = 0) = C_{r,0}$. Thus, the analytical solution, which is an infinite series, can be obtained as

$$C_r = C_{r,b} + \sum_{n=1}^{\infty} a_n \cdot e^{-b_n t} \cdot \cos(c_n x) \tag{13}$$

where $c_n = (n - 0.5)\pi/L_c$ ($n \geq 1$, and n is an integer), $b_n = D_e \cdot {c_n}^2$, and $a_n = C_{r,0} - C_{r,b}$.

In order to simplify the solution, only the first polynomial of (13), which means $n = 1$, is adopted. Thus, the average moisture content $C_{r,a}$ can be calculated, which is

$$\begin{aligned} C_{r,a} &= \frac{\int_0^{L_c} C_r dx}{L_c} \\ &= C_{r,b} + \frac{2(C_{r,0} - C_{r,b})}{\pi} \cdot e^{-(D_e \pi^2 / 4{L_c}^2)t} \end{aligned} \tag{14}$$

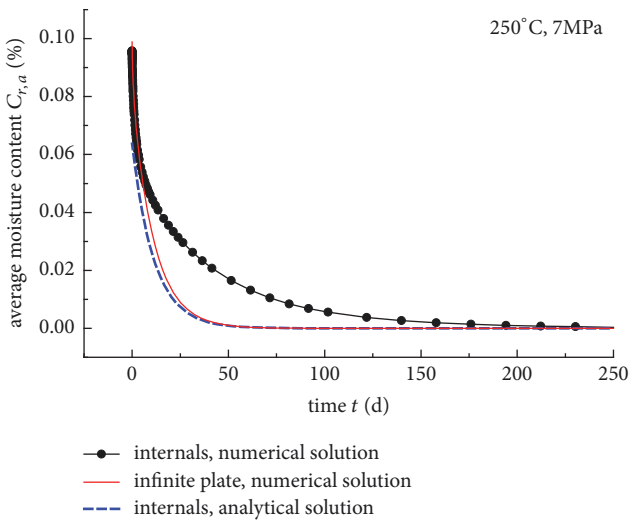

Figure 7: Comparison of analytical and numerical solutions.

As for the geometric model of internals of HTR-PM, according to the statistic obtained in Solidworks software, its L_c is 0.3066 m. In addition, considering $C_{r,b} = 0$ and $C_{r,0} = 0.1\%$, the analytical solution for dehumidification of HTR-PM can be obtained.

Figure 7 shows the comparison between analytical and numerical simulation. It is found that curves $C_{r,a}$-t of analytical and numerical solution of infinite plate are in good agreement. While comparing curves of analytical and numerical solution of HTR-PM, it is found that the agreement is not that good. It is suggested that the simplified analytical solution is pretty accurate for an ideal regular geometry model, while it is difficult to obtain the characteristic length L_c to accurately represent an irregular geometry. The uneven distribution of channels, chambers, and other irregular structures in reactor core results in the deviation of solution. It is also suggested that, in order to derive a more representative L_c, some optimization methods can be adopted to the calculation of L_c, e.g., introducing empirical correction coefficient, dividing the whole geometry into several sections, etc.

5. Conclusion

In the dehumidification process of HTGR, the major moisture transfer mechanism in carbon materials includes molecular diffusion and seepage. Thus, diffusion model and diffusion-seepage model are developed to describe the dehumidification process of internals in reactor core. The simulation result of dehumidification of HTR-PM suggests that the average moisture content of internals decreases exponentially with time and the moisture mainly concentrates in the top and bottom of core. According to the sensitivity analysis, the dehumidification efficiency can be promoted by the increase of temperature and decrease of system pressure, especially by reducing the system pressure, and the dehumidification efficiency can be greatly improved. The analysis on analytical solution of dehumidification problem shows that the simplified analytical solution is pretty accurate for an ideal regular geometry model, while the calculation of characteristic length of irregular geometry needs to be improved.

Data Availability

The data used to support the findings of this study are included within the article.

Conflicts of Interest

The authors declare that they have no conflicts of interest.

Acknowledgments

This work was supported by the National Natural Science Foundation of China (NSFC) (Grant no. 11302117), Beijing Natural Science Foundation (Grant no. 2182023), and the Chinese National S&T Major Project (Grant no. ZX06901).

References

[1] D. V. Ragone, W. V. Goeddel, and L. R. Zumwalt, "Graphite-matrix nuclear fuel systems for the peach bottom HTGR," *J. Annealing*, 1963.

[2] S. J. Xu and F. Y. Kang, *Carbon and Graphite Materials in Nuclear Engineering*, M. Tsinghua University Press, 2010.

[3] T. L. Albers, "High-Temperature Properties of Nuclear Graphite," *Journal of Engineering for Gas Turbines and Power*, vol. 131, no. 6, Article ID 064501, 2009.

[4] Z. Zhang, Z. Wu, Y. Sun, and F. Li, "Design aspects of the Chinese modular high-temperature gas-cooled reactor HTR-PM," *Nuclear Engineering and Design*, vol. 236, no. 5-6, pp. 485–490, 2006.

[5] L. S. Wang, Y. C. Fang, F. Wu et al., "The position of boron carbide in nutron absorbing materials and its properties relation to nuclear application," *J. Materials Science and Engineering of Powder Metallurgy*, vol. 2, pp. 113–120, 2000.

[6] Z. Zhang, J. Liu, S. He, Z. Zhang, and S. Yu, "Structural design of ceramic internals of HTR-10," *Nuclear Engineering and Design*, vol. 218, no. 1-3, pp. 123–136, 2002.

[7] X. Zhou, Y. Tang, Z. Lu, J. Zhang, and B. Liu, "Nuclear graphite for high temperature gas-cooled reactors," *New Carbon Materials*, vol. 32, no. 3, pp. 193–204, 2017.

[8] L. U. Zhen-ming, X. T. Chen, and L. Q. Wei, "Pore structure and moisture absorption property of carbon materials in HTR," *Journal of Atomic Energy Science and Technology*, vol. 50, no. 3, pp. 477–483, 2016.

[9] J. R. Morris, C. I. Contescu, M. F. Chisholm et al., "Modern approaches to studying gas adsorption in nanoporous carbons," *Journal of Materials Chemistry A*, vol. 1, no. 33, pp. 9341–9350, 2013.

[10] M. Steinbrück, "Oxidation of boron carbide at high temperatures," *Journal of Nuclear Materials*, vol. 336, no. 2-3, pp. 185–193, 2005.

[11] P. Wang, Y. Wang, and S. Y. YU, "Characterization of porosity development in oxidized nuclear graphite," *J. Science & Technology Review*, vol. 30, no. 20, pp. 21–26, 2012.

[12] R. P. Wichner, T. D. Burchell, and C. I. Contescu, "Penetration depth and transient oxidation of graphite by oxygen and water

vapor," *Journal of Nuclear Materials*, vol. 393, no. 3, pp. 518–521, 2009.

[13] C. I. Contescu, T. Guldan, P. Wang, and T. D. Burchell, "The effect of microstructure on air oxidation resistance of nuclear graphite," *Carbon*, vol. 50, no. 9, pp. 3354–3366, 2012.

[14] X. L. Yu, X. Y. Yang, and S. Y. YU, "Present status of research on the oxidation of graphite in case of air and water leakage in HTR," *Journal of Nuclear Power Engineering*, pp. 313–315, 2006.

[15] P. Wang, C. I. Contescu, S. Yu, and T. D. Burchell, "Pore structure development in oxidized IG-110 nuclear graphite," *Journal of Nuclear Materials*, vol. 430, no. 1-3, pp. 229–238, 2012.

[16] X.-L. Yu, X.-W. Luo, and S.-Y. Yu, "Simulation of oxidation in HTR-10 core," *Hedongli Gongcheng/Nuclear Power Engineering*, vol. 31, no. 2, pp. 81–97, 2010.

[17] J. Y. Dou and H. Q. Yin, "Preliminary investigation into the dehumidification model of HTR-PM initial core," in *Proceedings of the 14th National Symposium on Reactor Thermal Fluid*, Beijing, China, 2015.

[18] X. D. Liu and B. B. Yang, "Review and vista on drying theories of porous medium," *Journal of China Agricultural University*, vol. 10, no. 4, pp. 81–92, 2005.

[19] W. Xu, L. SHI, Y. H. Zheng et al., "Research on oxidation model of nuclear grade graphite IG-110," *Journal of Atomic Energy Science and Technology*, vol. 49, pp. 475–480, 2015.

[20] P. Wang and S. Y. Yu, "Study on model of nuclear graphite oxidation," *Journal of Atomic Energy Science and Technology*, vol. 46, no. 1, pp. 84–88, 2012.

[21] Z. Chen, P. Zhou, and C. Mei, "Principle of transportation processes," *M. Central*, pp. 333–337, 2011.

[22] Z. S. Ji, R. K. Zhu, and D. Li, *Principle of transmission*, M. Harbin Institute of Technology Press, Harbin, China, 2002.

[23] F. H. Clarke, R. J. Stern, and P. R. Wolenski, "Proximal smoothness and the lower C2 property," *Journal of Convex Analysis*, vol. 2, no. 1, pp. 117–144, 1995.

[24] Q. Liu and Y. F. Hu, *Study on Non-linear Seepage Flow Law in Carbon Graphite and Impregnated Antimony Experimental Analysis*, D. China Mining University, Xuzhoum, China, 2010.

[25] L. Kong, *Engineering Fluid Mechanics*, vol. 7, M. China Electric Power Press, Beijing, China, 2010.